

1 **Investigations of Aerobic Methane Oxidation in Two Marine Seep**
2 **Environments Part 2: Isotopic Kinetics**

3

4 **E. W. Chan¹, A. M. Shiller², D. J. Joung², E. C. Arrington³, D. L. Valentine⁴, M. C.**
5 **Redmond⁵, J. A. Breier⁶, S. A. Socolofsky⁷, J. D. Kessler¹**

6 ¹Earth and Environmental Sciences, University of Rochester, Rochester, NY 14627, USA

7 ²Division of Marine Science, University of Southern Mississippi, Stennis Space Center,
8 MS 39529, USA

9 ³Interdepartmental Graduate Program in Marine Science, University of California – Santa
10 Barbara, Santa Barbara, CA 93106, USA

11 ⁴Dept. of Earth Science and Marine Science Institute, University of California – Santa
12 Barbara, Santa Barbara, CA 93106, USA

13 ⁵Dept. of Biological Sciences, University of North Carolina Charlotte, Charlotte, NC
14 28223, USA

15 ⁶School of Earth, Environment, and Marine Sciences, University of Texas Rio Grande
16 Valley, Brownsville, TX 78597 USA

17 ⁷Zachry Dept. of Civil Engineering, Texas A&M University, College Station, TX 77843
18 USA

19

20 Corresponding authors: Eric Chan (erik.w.chan@gmail.com) and John Kessler
21 (john.kessler@rochester.edu)

22

23 **Key Points:**

24 • Systematic seawater incubations were conducted to determine stable isotopic
25 changes associated with aerobic methane oxidation.

26 • Isotopic fractionation caused by aerobic methane oxidation was shown to follow
27 first-order isotopic kinetics.

28 • Despite displaying a microbial bloom associated with rapid oxidation events, the
29 isotopic fractionation factor remained constant.

30

31 **Abstract**

32 During aerobic oxidation of methane (CH_4) in seawater, a process which mitigates
33 atmospheric emissions, the ^{12}C -isotopologue reacts with a slightly greater rate constant
34 than the ^{13}C -isotopologue, leaving the residual CH_4 isotopically fractionated. Prior
35 studies have attempted to exploit this systematic isotopic fractionation from methane
36 oxidation to quantify the extent that a CH_4 pool has been oxidized in seawater. However,
37 cultivation-based studies have suggested that isotopic fractionation fundamentally
38 changes as a microbial population blooms in response to an influx of reactive substrates.
39 Using a systematic mesocosm incubation study with recently collected seawater, here we
40 investigate the fundamental isotopic kinetics of aerobic CH_4 oxidation during a microbial
41 bloom. As detailed in a companion paper, seawater samples were collected from seep
42 fields in Hudson Canyon, US Atlantic Margin and atop Woolsey Mound (a.k.a. Sleeping
43 Dragon) which is part of lease block MC118 in the northern Gulf of Mexico, and used in
44 these investigations. The results from both Hudson Canyon and MC118 show that in
45 these natural environments isotopic fraction for CH_4 oxidation follows a first-order
46 kinetic process. The results also show that the isotopic fractionation factor remains
47 constant during this methanotrophic bloom once rapid CH_4 oxidation begins and that the
48 magnitude of the fractionation factor appears correlated with the first-order reaction rate
49 constant. These findings greatly simplify the use of natural stable isotope changes in CH_4
50 to assess the extent that CH_4 is oxidized in seawater following seafloor release.

51

52 **Plain Language Summary**

53 The aerobic oxidation of methane in seawater is a process that prevents methane
54 produced in the oceanic environment from being emitted to the atmosphere. During this
55 process, isotopic forms of methane are oxidized at slightly different rates leading to
56 changes in the natural methane isotope ratios with the extent of oxidation. While these
57 changes in isotope ratios would seem to be a proxy for the extent of methane oxidation,
58 laboratory-based studies involving pure cultures have shown that these isotope ratio
59 changes vary as a microbial population blooms in response to an increase in substrates.
60 This study systematically measured the stable isotope changes that are associated with
61 aerobic methane oxidation in recently collected seawater collected from regions of active
62 seafloor methane release along the U.S. Atlantic margin and the Gulf of Mexico. Results
63 show that these isotope changes are systematic during methane oxidation, greatly
64 simplifying the use of isotope changes to determine the extent of methane oxidation.

65 **1. Introduction**

66 Kinetic processes, such as microbial oxidation, are known to systematically change the
67 isotopic abundance of various molecules. Typically, the light isotopologue reacts with a
68 slightly faster rate constant than the heavy isotope, leaving the residual reactant
69 isotopically fractionated. For example, studies of oceanic methane (CH_4) have utilized
70 this isotopic fractionation as a proxy for the extent of CH_4 oxidation and have gone so far

71 as to use it to help determine oxidation rates (e.g., Kessler et al., 2006; Leonte et al.,
72 2017). The oceanic CH₄ reservoir is one of the largest CH₄ reservoirs on Earth, and
73 significant releases of CH₄ from the seafloor into the overlying waters have been
74 documented in the modern ocean (Ruppel and Kessler, 2017). However, the minimal
75 emission of oceanic CH₄ to the atmosphere (Dlugokencky et al., 2011) underscores active
76 CH₄ oxidation in seawater and surface sediments that prevents atmospheric release.

77 Traditionally, CH₄ oxidation rates are not measured using natural stable isotope changes.
78 Instead, CH₄ oxidation rate measurements are generally conducted by collecting seawater
79 samples in glass vials, inoculating the samples with radioactive or stable isotopically-
80 labeled CH₄ immediately after collection, incubating at in-situ temperatures for a
81 measured time period, and terminating further oxidation with the addition of a toxic agent
82 such as mercuric chloride (e.g. Crespo-Medina et al., 2014; Mendes et al., 2015;
83 Niemann et al., 2015; Pack et al., 2011 and 2015; Valentine et al., 2001; Valentine et al.,
84 2010). The labeled CH₄ allows for tracing the reactant as it is incorporated into product
85 by native methanotrophs. Beyond not maintaining in-situ pressures, a consistent
86 challenge with these techniques is amending the seawater sample while minimizing the
87 disturbance to the natural concentrations of the dissolved gases (Pack et al., 2011), trace
88 metals, and nutrients. Typically, these studies involve multiple samples per rate
89 determination that are often collected in different glass vials and not allowed to incubate
90 in the same reservoir (e.g. Crespo-Medina et al., 2014; Leonte et al., 2017; Mendes et al.,
91 2015; Pack et al., 2011). This creates individual samples - pseudoreplicates - that might
92 proceed at differing oxidation rates due to slight differences in initial microbial
93 populations or in dissolved gases and substrates (e.g., nutrients and trace metals) utilized
94 in the oxidation processes. Further adding to complications, borosilicate glass serum vials
95 that are traditionally used for CH₄ oxidation rate measurements have been shown to leach
96 trace metals (e.g., Fe and Cu) from the borosilicate glass, potentially fertilizing the
97 samples with greater amounts of essential trace metals than occur naturally (Batley and
98 Gardner, 1977; Robertson, 1968). Additionally, certain rubber stoppers used to seal these
99 vials have been shown to have toxic effects on methanotrophs (Niemann et al., 2015).

100 An alternative to using isotopic labeling techniques for measuring CH₄ oxidation rates is
101 the use of naturally occurring stable isotopes (Leonte et al., 2017). Recent advances in
102 technology enable these measurements to be conducted at sea and in-situ (Chen et al.,
103 2013; Wankel et al., 2012). A strong advantage with this approach is that integrated CH₄
104 oxidation rates are determined based on the in-situ isotopic conditions without the need to
105 externally incubate samples, which can potentially cause alterations to biological,
106 chemical, temperature, and pressure conditions (Leonte et al., 2017). During CH₄
107 oxidation, ¹²CH₄ is oxidized with a slightly greater rate constant than ¹³CH₄, causing the
108 residual CH₄ pool to become relatively enriched in the heavy isotopes over time
109 (Whiticar, 1999). Similarly, the lighter ¹²C of the oxidized CH₄ has been traced into the
110 products of cellular biomass and CO₂ (Orphan et al., 2001; Radajewski et al., 2000;
111 Summons et al., 1994). This isotopic fractionation process can be used to quantify the
112 extent of CH₄ oxidation if the fractionation factor (α) is known or can be determined

(Leonte et al., 2017). The α is the ratio of the rate constants of the lighter isotope over the heavy isotope assuming first-order kinetics for this oxidation process. Interestingly, culture studies of methane-producing archaea have reported that the fractionation factor changes during microbially mediated reactions as the microbial population grows (Botz et al., 1996; Penning et al., 2005; Valentine et al., 2004), potentially complicating the use of natural isotopes and isotopic fractionation to quantify CH₄ oxidation in natural environments that are not in steady-state conditions. This complication would be especially noticeable in environments where the dissolved CH₄ concentration rapidly increased in a parcel of water, such as a seep field or hydrocarbon spill (e.g. Kessler et al., 2011; Leonte et al., 2017), resulting in a significant bloom of the CH₄-oxidizing population. This proxy would only be quantitative during a microbial bloom/oxidation event once CH₄ oxidation isotopic fractionation factors stabilized. Thus, this study was motivated by the need to thoroughly quantify the changes in stable isotope kinetics as a population of methanotrophic bacteria grew to oxidize an enhanced CH₄ input.

Here we conducted mesocosm experiments with CH₄-laden seawater measuring isotopic changes over time during CH₄ oxidation events. The goal of this investigation was to determine fundamental stable isotopic fractionation parameters associated with aerobic CH₄ oxidation. To assess potential regional variabilities in CH₄ oxidation kinetics, seawater was collected in two different locations where CH₄ bubbles were seeping from the seafloor: a) Hudson Canyon off the coast of New York and New Jersey near the upper limit of CH₄ hydrate stability and b) the deep Gulf of Mexico near waters once impacted by the Deepwater Horizon blowout. The results of these studies can be used to help quantify the extent and rates of CH₄ oxidation based on natural changes of CH₄ isotopes.

2. Materials and Methods

All information relating to the seawater sample collection, incubation, and analysis can be found in the companion paper (Chan et al., submitted). To briefly summarize, waters directly influenced by, or adjacent to, known CH₄ seep activity were chosen to examine CH₄ oxidation kinetics. The first research expedition was aboard the R/V *Endeavor* along the North Atlantic Bight from 7-12 July 2014. The recently discovered CH₄ seeps off the coast of New York and New Jersey in Hudson Canyon (HC) (Rona et al., 2015; Skarke et al., 2014; Weinstein et al., 2016) provided an appropriate site for these experiments. Water samples were collected both inside the seep field (39° 32.705'N, 72° 24.259'W) as well as outside of HC in waters not directly impacted by CH₄ seeps (39° 17.236'N 72° 12.080'W), as determined by the presence or absence of acoustically detected bubbles (Leonte et al., 2017; Weinstein et al., 2016). These water samples were collected via Niskin bottles that were pre-cleaned for trace-metal analyses. A measured amount (150 ± 1.5 mL) of isotopically standardized CH₄ ($\delta^{13}\text{C-CH}_4 = -20\text{ ‰}$; Kessler and Reeburgh (2005)) was systemically added to each sample using a mass flow controller and gas filter apparatus to increase dissolved CH₄ concentrations to ca. 300 μM CH₄. Therefore, these mesocosm incubations using waters collected from the HC region began with similar values for dissolved CH₄ concentration and $\delta^{13}\text{C-CH}_4$.

154 A second research expedition was conducted from 9-20 April 2015 aboard the E/V
155 *Nautilus* at the Sleeping Dragon seep field site (MC118) in the Gulf of Mexico. MC118 is
156 17 km from the Deepwater Horizon (DWH) wellhead and provided physical-chemical
157 conditions similar to what may have been experienced during the DWH hydrocarbon spill
158 in 2010. The Suspended-Particle Rosette (SUPR) sampler (Breier et al., 2009) was
159 mounted to the ROV *Hercules* and was used for the high precision collection of water
160 that was visibly impacted by CH₄ bubbles. This sampling strategy enabled water to be
161 collected that contained naturally high concentrations of dissolved CH₄, so no additional
162 CH₄ was added. The results obtained from HC and MC118 were analyzed to determine
163 regional similarities and variabilities in CH₄ oxidation kinetics.

164 Full details of the sample collection, analysis, and calibration procedures can be found in
165 the companion paper (Chan et al., submitted). In addition, the specific details and
166 validation tests for the system used to incubate and analyze these mesocosms are
167 presented in Chan et al. (2016). Finally, all data and descriptions of the analyses from
168 these experiments are available through the Gulf of Mexico Research Initiative
169 Information & Data Cooperative (GRIIDC) (Kessler and Chan, 2017).

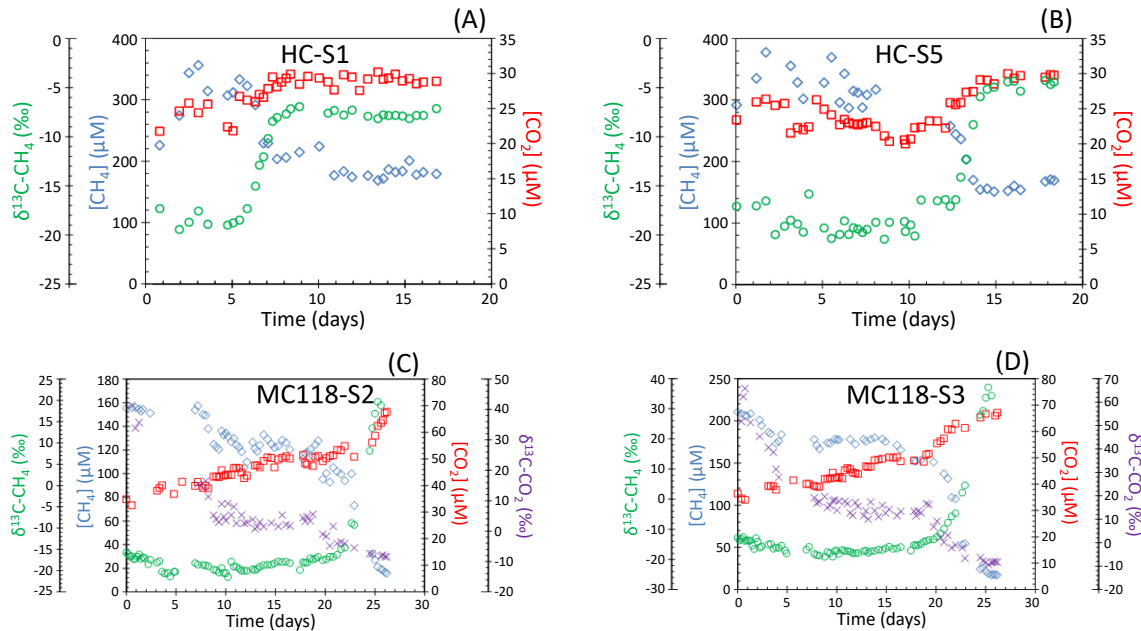
170

171 **3. Results and Discussion**

172 **3.1. General Stable Isotope Changes**

173 Every incubation experiment was examined to determine whether clear signs of aerobic
174 CH₄ oxidation had occurred by comparing changes in dissolved gas concentrations,
175 isotope measurements, microbial community, cell densities, and micro- and macro-
176 nutrients (see companion paper for complimentary analyses). Six of the ten mesocosms
177 with waters collected inside and adjacent to HC exhibited CH₄ oxidation (Figures 1A-B
178 and S1). Four of the ten mesocosms collected with waters at MC118 displayed clear
179 characteristics of CH₄ oxidation (Figures 1C-D and S3-S4). While we do not have clear
180 evidence to explain this observation, we offer two possibilities. First, the mesocosms may
181 have grown successfully but a partial blockage in the water sampling tubes may have
182 prevented accurate measurements. Second, the process of removing the samples from
183 their deep ocean environment may have harmed the indigenous population.

184



185
186 **Figure 1.** Dissolved concentrations of CH_4 (blue diamonds), CO_2 (red squares), $\delta^{13}\text{C-CH}_4$ (green circles) (Chan et al., submitted), and $\delta^{13}\text{C-CO}_2$ (purple \times) over the course of
187 the incubations. (A) HC-S1 (on seep), (B) HC-S5 (off seep), (C) MC118-S2 (on seep)
188 and (D) MC118-S3 (on seep). All data in these figures is available through the Gulf of
189 Mexico Research Initiative Information & Data Cooperative (GRIIDC) (Kessler and
190 Chan, 2017).
191

193 Along with the measurement of the changes in chemical concentrations and microbial
194 populations (see companion paper), $\delta^{13}\text{C-CH}_4$ and $\delta^{13}\text{C-CO}_2$ were measured using real-
195 time monitoring to assess microbial isotopic fractionation of the substrate and product.
196 Since the HC samples were equilibrated with standardized CH_4 , these incubations began
197 close to the $\delta^{13}\text{C-CH}_4$ standardized value of -20 ‰ (Chan et al., submitted; Kessler and
198 Reeburgh, 2005). The HC mesocosms showed an average change in $\delta^{13}\text{C-CH}_4$ of 11 ± 1
199 ‰ to more positive (heavier) values (Figures 1 and S1, Table S1). The measurement of
200 $\delta^{13}\text{C-CO}_2$ was unsuccessful for the HC mesocosms due to a manifold failure; however,
201 the system was redesigned for the MC118 experiments producing usable results.

202 The starting $\delta^{13}\text{C-CH}_4$ for MC118 varied based on the natural input of dissolved CH_4
203 supplied by the Sleeping Dragon seep. The average starting $\delta^{13}\text{C-CH}_4$ was approximately
204 -28 ± 11 ‰ and for those samples exhibiting oxidation, the average increase in $\delta^{13}\text{C-CH}_4$
205 was 37 ± 15 ‰ (Figures 1, S3, and S4, and Table S1). Additionally, CO_2 became more
206 depleted in ^{13}C over time with an average change of -10 ± 10 ‰ (Figure S4 and Table
207 S1). These isotopic shifts ($\delta^{13}\text{C-CH}_4$ to heavier values and $\delta^{13}\text{C-CO}_2$ to lighter values)
208 throughout these incubations suggest that CH_4 oxidation is occurring and transferring
209 carbon from the dissolved CH_4 pool to the dissolved CO_2 pool.

210

211 **3.2. Fractionation Factor (α) for Aerobic CH₄ Oxidation**212 The isotopic fractionation factor (α) is a constant describing the extent that isotopes of
213 one compound change during a kinetic process, fundamentally defined in this experiment
214 as the ratio of the first-order rate constants for the oxidation of ¹²CH₄ over ¹³CH₄ (Eq. 1).

215
$$\alpha = k_{12c}/k_{13c} \quad (\text{Eq. 1})$$

216 where k is the first-order rate constant with units of day⁻¹ such that,

217 Rate = $k[\text{CH}_4] \quad (\text{Eq. 2})$

219 and [CH₄] is dissolved CH₄ concentration.

220

221 Since the mesocosm incubations are closed-system experiments, not allowing for the
222 addition or loss of reactants or products to the outside environment, isotopic fractionation
223 can be modeled with the Rayleigh equation (Bigeleisen and Wolfsberg, 1958). This
224 allows for calculating α using a method previously outlined in Leonte et al. (2017). This
225 method linearizes the Rayleigh equation and determines α from the slope of the linearized
226 data (Eq. 3).

227
$$\ln[\text{CH}_4] = \frac{\alpha}{1-\alpha} * \ln[\delta R + 1000] - \frac{\alpha}{1-\alpha} * \ln[\delta R_0 + 1000] + \ln[\text{CH}_{4,0}] \quad (\text{Eq. 3})$$

228 Here, [CH₄] is the dissolved CH₄ concentration, [CH_{4,0}] is the dissolved CH₄
229 concentration at the start of the reaction, δR is ¹³C-CH₄, and δR_0 is ¹³C-CH₄ at the start
230 of the reaction. The slope of $\ln[\text{CH}_4]$ vs. $\ln[\delta R + 1000]$ is $\alpha/(1-\alpha)$, which can be
231 rearranged to determine α (Leonte et al., 2017). The geometric mean regression is used
232 here when determining the linear regression between $\ln[\text{CH}_4]$ and $\ln[\delta R + 1000]$ because
233 it takes into account uncertainty in both variables.234 The average α for the mesocosms collected in the HC over the seep field was $1.023 \pm$
235 0.003 . The MC118 mesocosms produced an average α of 1.022 ± 0.003 , which is
236 statistically similar to the values obtained directly in the seep field in HC. However, α
237 was different for the experiments utilizing water that was not directly impacted by CH₄
238 bubbles released from a seep field, displaying an average $\alpha = 1.04 \pm 0.01$. In addition to
239 displaying a higher average α , the HC mesocosms using water collected outside the seep
240 field also displayed lower average rate constants (see companion paper), supporting the
241 conclusion that slower rates of CH₄ oxidation produce larger fractionation factors (Table
242 1; Figure 2). Viewed differently, larger oxidation rate constants cause lower degrees of
243 isotopic fraction, a conclusion which can be used to predict the largest oxidation rate
244 constant which would ultimately produce no isotopic fractionation (i.e., $\alpha = 1$). To
245 constrain this endmember, we calculated a linear regression between k and α again using

246 a geometric mean regression since it takes into account uncertainty in both variables
 247 (Figure 2). This regression predicts a maximum rate constant (k_{\max}) of 0.44 day^{-1} to
 248 produce no isotopic fractionation. However, this conclusion is rather uncertain ($k_{\max} =$
 249 $0.44 \pm 3.9 \text{ day}^{-1}$) when the uncertainties in both the slope and y-intercept of the geometric
 250 mean regression ($k = (-9.3 \pm 2.7)\alpha + (9.8 \pm 2.8)$) are propagated. Nonetheless, it is
 251 interesting to note the similarities between this maximum rate constant which would
 252 produce no isotopic fraction and the rate constants measured during and after the DWH
 253 blowout (Figure 2, and Figure 1 in Chan et al., submitted).

254 **Table 1.** The characteristics for isotopic kinetics determined in Hudson Canyon (HC) and
 255 MC118. The units for the first-order oxidation rate constants (k) is day^{-1} and isotopic
 256 fractionation factors (α) in unitless ($\text{day}^{-1/2} \text{ day}^{-1}$).

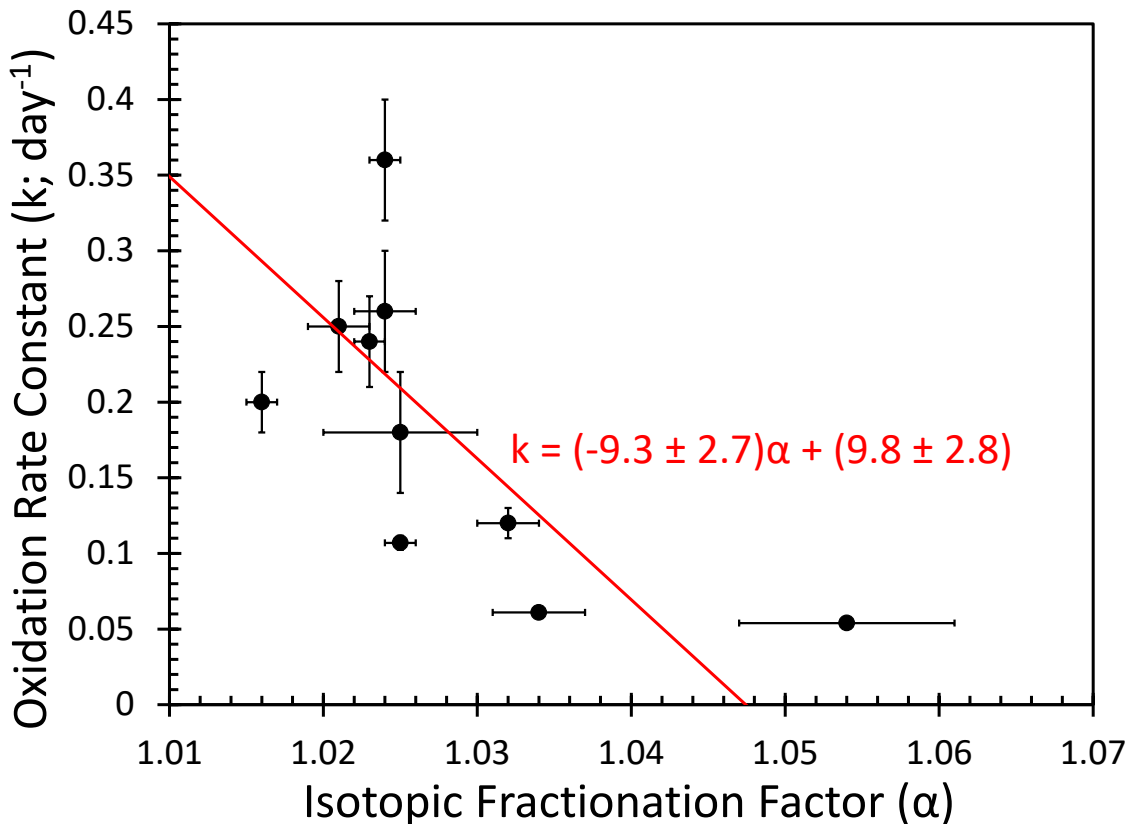
257

Sample	Location	$k (\text{day}^{-1})$	α
HC-S1	On seep	0.25 ± 0.03	1.021 ± 0.002
HC-S2	On seep	0.18 ± 0.04	1.025 ± 0.005
Average	On seep	0.22 ± 0.05	1.023 ± 0.003
HC-S3	Off seep	0.054 ± 0.004	1.054 ± 0.007
HC-S4	Off seep	0.12 ± 0.01	1.032 ± 0.002
HC-S5	Off seep	0.24 ± 0.03	1.023 ± 0.001
HC-S6	Off seep	0.061 ± 0.003	1.034 ± 0.003
Average:	Off seep	0.12 ± 0.09	1.04 ± 0.01
MC118-S1	On seep	0.107 ± 0.005	1.025 ± 0.001
MC118-S2	On seep	0.26 ± 0.04	1.024 ± 0.002
MC118-S3	On seep	0.36 ± 0.04	1.024 ± 0.001
MC118-S4	On seep	0.20 ± 0.02	1.016 ± 0.001
Average:	On seep	0.2 ± 0.1	1.022 ± 0.004

258

259

260



261
262

263 **Figure 2.** The first-order rate constant (k) for aerobic CH₄ oxidation as a function of
264 isotopic fractionation factor (α) for δ¹³C-CH₄. The linear regression was determined using
265 the Geometric Mean to consider the uncertainties in both the rate constant and isotopic
266 fractionation factor.

267 3.3. Isotopic Fraction with the Stage of Microbial Growth

268 Previous studies have collected data from laboratory cultures of methanogens suggesting that
269 isotopic fractionation factors change with the stage of microbial growth (Botz et al., 1996;
270 Penning et al., 2005; Valentine et al., 2004). If applicable to aerobic methanotrophs, the use of
271 natural stable isotopes to determine the extent of CH₄ oxidation (e.g., Leonte et al., 2017) would
272 be significantly more complicated, if not impossible. Not only would the fractionation factor
273 need to be known, but also how it changes with the stage of microbial growth and the stage of
274 microbial growth in the natural environment at the time of sampling.

275 Here we test if the isotopic fractionation factor changed throughout rapid CH₄ oxidation. To do
276 so, we isolated the data between the start and conclusion of rapid CH₄ oxidation (Kessler and
277 Chan, 2017) and fit the data with the closed-system Rayleigh isotope fractionation model (Eq. 4),
278 as was described previously (Leonte et al., 2017).

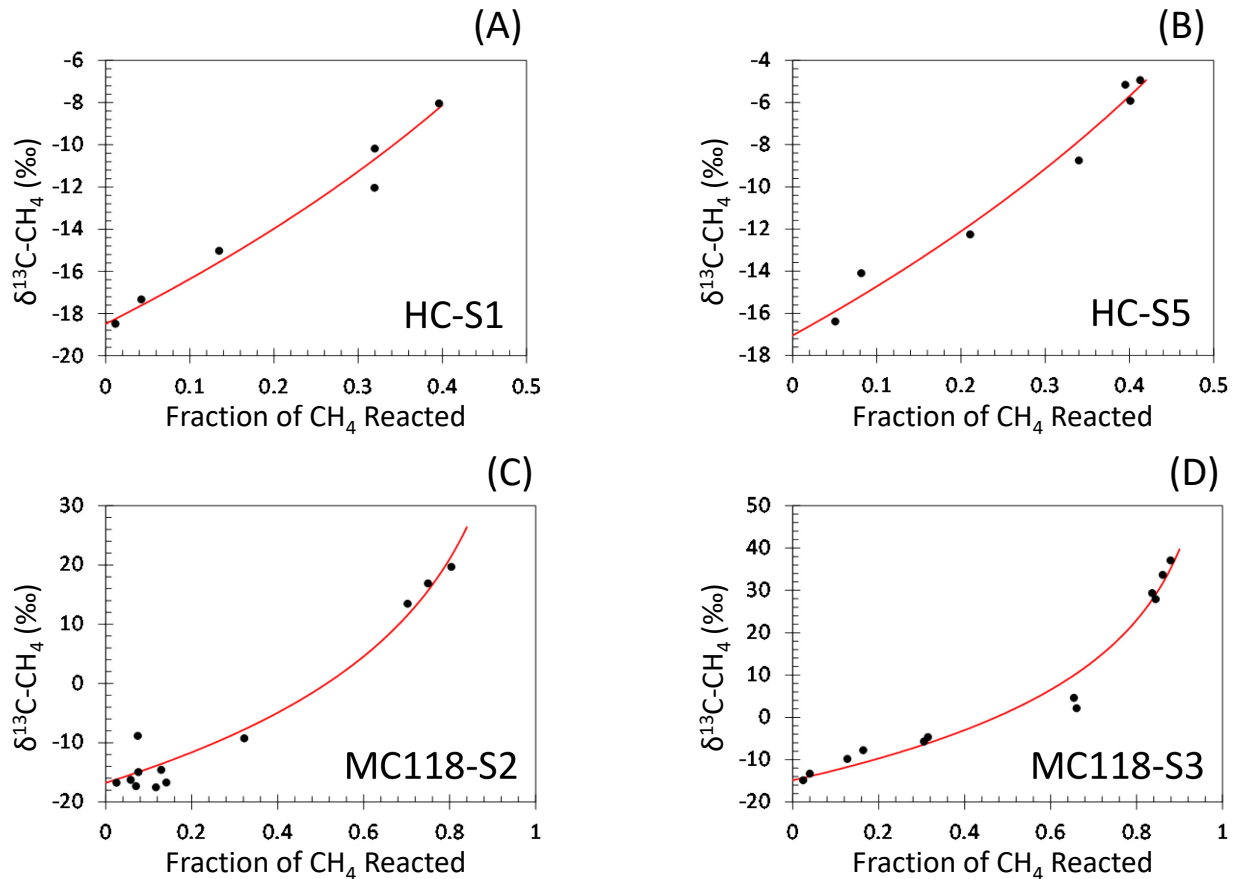
279

$$280 \delta R = (\delta R_0 + 1000)(1 - f)^{1/\alpha-1} - 1000 \quad (\text{Eq. 4})$$

281 The variables of δR , δR_0 , and α are as defined above, while f is the fraction of CH₄ that is
282 oxidized. More specifically, $f = 1 - C/C_0$, where C is the measured [CH₄] and C_0 is the average
283 concentration of dissolved CH₄ at the start of rapid CH₄ oxidation (Leonte et al., 2017).

284 While the previous experiments that displayed a change in isotopic fractionation factor with the
285 stage of microbial growth involved open-system pure cultures of methanogens (Botz et al., 1996;
286 Penning et al., 2005), our data from these closed-system mesocosm experiments investigating
287 methanotrophy could be modeled with a constant isotopic fractionation factor after rapid CH₄
288 oxidation initiated (Figures 3, S2, and S5), despite large changes in microbial biomass (see
289 companion paper). This result greatly simplifies the use of natural stable isotope changes in
290 seawater to determine the extent of aerobic oxidation since only one fractionation factor is
291 necessary to estimate the extent of CH₄ oxidation (e.g. Leonte et al., 2017).

292



296
 297 **Figure 3.** Values of $\delta^{13}\text{C-CH}_4$ plotted as a function of the fraction of CH_4 reacted in these
 298 mesocosm experiments. The model (red curve) fits the measurements (black dots) when a
 299 constant isotopic fractionation is considered (Table 1). The model incorporates the closed-system
 300 Rayleigh approach (Eq. 4) and an average CH_4 concentration at the start of rapid CH_4 oxidation,
 301 as described previously (Leonte et al., 2017).

302 4. Conclusions

303 Measurements of natural $\delta^{13}\text{C-CH}_4$ in seawater are a powerful tool to assess the extent of aerobic
 304 oxidation. Following seafloor release and dissolution into the overlying waters, CH_4 can either
 305 be oxidized by indigenous microorganisms or diluted prior to atmospheric emission. While both
 306 oxidation and dilution decrease the initial dissolved CH_4 concentration, only oxidation
 307 systematically changes the natural $\delta^{13}\text{C-CH}_4$. Here, we investigated the stable isotope kinetics of
 308 aerobic CH_4 oxidation using mesocosm incubations of seawater collected in two seep fields, one
 309 in the North Atlantic Bight in and near Hudson Canyon and the other in the Gulf of Mexico. The
 310 results produced from these experiments led to three conclusions regarding the fundamental
 311 isotope kinetics of aerobic CH_4 oxidation. First, the isotope data is best modeled with the
 312 Rayleigh model, an isotope model for a closed-system following first-order reaction kinetics.
 313 Second, the fractionation factor produced was correlated with the overall reaction rate constant.
 314 Reactions with larger rate constants had smaller fractionation factors and vice versa. While the
 315 isotopic fractionation factors were different between on-seep and off-seep waters at HC, the

316 isotopic fractionation factors were similar when using waters directly impacted by CH₄ seeps,
317 regardless of oceanic location. Third, despite a large increase in microbial biomass during these
318 oxidation experiments and previous reports concluding that isotope fractionation factors changed
319 with the stage of microbial growth, the results here indicate that the fractionation factor remained
320 constant throughout these oxidation events. These fundamental results are encouraging, as they
321 suggest that the extent of CH₄ oxidation can be determined using traditional isotopic
322 fractionation equations without regard to the stage of microbial growth so long as the
323 fractionation factor can be determined for that specific environment.

324

325

326

327 **Acknowledgements**

328 This work was made possible by grants from the National Science Foundation (OCE-1318102 to
329 J.D.K.) and the Gulf of Mexico Research Initiative through the GISR (to J.D.K.) and
330 CONCORDE (to A.M.S.) consortia. Support for D.L.V. and E.C.A. also came primarily from
331 OCE-1318102, but secondary support was provided by the NSF (OCE-1333162 and OCE-
332 1756947). Data are publicly available through the Gulf of Mexico Research Initiative
333 Information & Data Cooperative (GRIIDC) at
334 <https://data.gulfresearchinitiative.org/data/R1.x137.000:0019>. We thank the captain and crew of
335 the R/V *Endeavor* and the E/V *Nautilus* as well as Bill Fanning and Nicole Raineault for their
336 enthusiasm and support at sea. Finally, we would like to thank Patrick Crill, an anonymous
337 reviewer, and the editor for constructive suggestions which helped to strengthen this manuscript.

338

339 **References**

340

341 Batley, G. E., & Gardner, D. (1977). Sampling and storage of natural waters for trace metal
342 analysis. *Water Research*, 11(9), 745-756. [https://doi.org/10.1016/0043-1354\(77\)90042-2](https://doi.org/10.1016/0043-1354(77)90042-2)

343 Bigeleisen, J., & Wolfsberg, M. (1958). *Advances in Chemical Physics*, 1, 15-76.

344 Botz, R., Pokojski, H. D., Schmitt, M., & Thomm, M. (1996). Carbon isotope fractionation
345 during bacterial methanogenesis by CO₂ reduction. *Organic Geochemistry*, 25(3-4), 255-262.
346 [https://doi.org/10.1016/S0146-6380\(96\)00129-5](https://doi.org/10.1016/S0146-6380(96)00129-5)

347 Breier, J. A., Rauch, C. G., McCartney, K., Toner, B. M., Fakra, S. C., White, S. N., & German,
348 C. R. (2009). A suspended-particle rosette multi-sampler for discrete biogeochemical sampling
349 in low-particle-density waters. *Deep Sea Research Part I: Oceanographic Research Papers*,
350 56(9), 1579-1589. <https://doi.org/10.1016/j.dsr.2009.04.005>

351 Chan, E. W., Kessler, J. D., Shiller, A. M., Joung, D. J., & Colombo, F. (2016). Aqueous
352 Mesocosm Techniques Enabling the Real-Time Measurement of the Chemical and Isotopic
353 Kinetics of Dissolved Methane and Carbon Dioxide. *Environmental Science & Technology*,
354 50(6), 3039-3046. <https://doi.org/10.1021/acs.est.5b04304>

355 Chen, Y., Lehmann, K., Kessler, J. D., Sherwood Lollar, B., Lacrampe Couloume, G., & Onstott,
356 T. C. (2013). Measurement of the ¹³C/¹²C of Atmospheric CH₄ Using Near-IR (NIR) Cavity
357 Ring-Down Spectroscopy. *Analytical Chemistry*, 85(23), 11250-11257.
358 <https://doi.org/10.1021/ac401605s>

359 Crespo-Medina, M., Meile, C. D., Hunter, K. S., Diercks, A-R., Asper, V. L., Orphan, V. J., et al.
360 (2014). The rise and fall of methanotrophy following a deepwater oil-well blowout. *Nature
361 Geoscience*, 7(6), 423-427. <https://doi.org/10.1038/NGEO2156>

362 Dlugokencky, E. J., E. G. Nisbet, R. Fisher, & D. Lowry (2011). Global atmospheric methane:
363 budget, changes and dangers. *Philosophical Transactions of the Royal Society of London A:
364 Mathematical, Physical and Engineering Sciences*, 369(1943), 2058-2072.
365 <https://doi.org/10.1098/rsta.2010.0341>

366 Kessler, J. D., & Chan, E. (2017). Chemical and Isotopic Kinetics of Dissolved Methane and
367 Carbon Dioxide for samples collected in the northern Gulf of Mexico and Atlantic July 2014-
368 April 2015. Distributed by Gulf of Mexico Research Initiative Information and Data Cooperative
369 (GRIIDC), Harte Res. Inst., Texas A&M Univ., Corpus Christi, Corpus Christi,
370 <https://doi.org/10.7266/N7RR1WPX>

371 Kessler, J. D., Valentine, D. L., Redmond, M. C., Du, M., Chan, E.W., Mendes, S.D., et al.
372 (2011). A Persistent Oxygen Anomaly Reveals the Fate of Spilled Methane in the Deep Gulf of
373 Mexico. *Science*, 331(6015), 312-315. <https://doi.org/10.1126/science.1199697>

374 Leonte, M., Kessler, J. D., Kellermann, M. Y., Arrington, E. C., Valentine, D. L., & Sylva, S. P.
375 (2017). Rapid rates of aerobic methane oxidation at the feather edge of gas hydrate stability in

376 the waters of Hudson Canyon, US Atlantic Margin. *Geochimica et. Cosmochimica Acta*, 204,
377 375-387. <https://doi.org/10.1016/j.gca.2017.01.009>

378 Mendes, S. D., Redmond, M. C., Voigritter, K., Perez, C., Scarlett, R., & Valentine, D. L.
379 (2015). Marine microbes rapidly adapt to consume ethane, propane, and butane within the
380 dissolved hydrocarbon plume of a natural seep. *Journal of Geophysical Research: Oceans*,
381 120(3), 1937-1953. <https://doi.org/10.1002/2014JC010362>

382 Niemann, H., Steinle, L., Blees, J., Bussmann, I., Treude, T., Krause, S., Elvert, M., & Lehmann,
383 M. F. (2015). Toxic effects of lab-grade butyl rubber stoppers on aerobic methane oxidation.
384 *Limnology and Oceanography: Methods*, 13(1), 40-52. <https://doi.org/10.1002/lom3.10005>

385 Orphan, V., Hinrichs, K.-U., Ussler, W., Paull, C. K., Taylor, L., Sylva, S. P., Hayes, J. M., &
386 DeLong, E. F. (2001). Comparative analysis of methane-oxidizing archaea and sulfate-reducing
387 bacteria in anoxic marine sediments. *Applied and Environmental Microbiology*, 67(4), 1922-
388 1934. <https://doi.org/10.1128/AEM.67.4.1922-1934.2001>

389 Pack, M. A., Heintz, M. B., Reeburgh, W. S., Trumbore, S. E., Valentine, D. L., Xu, X., &
390 Druffel, E. R. M. (2011). A method for measuring methane oxidation rates using lowlevels of
391 ¹⁴C-labeled methane and accelerator mass spectrometry. *Limnology and Oceanography:*
392 *Methods*, 9, 245-260. <https://doi.org/10.4319/lom.2011.9.245>

393 Pack, M. A., Heintz, M. B., Reeburgh, W. S., Trumbore, S. E., Valentine, D. L., Xu, X., &
394 Druffel, E. R. M. (2015). Methane oxidation in the eastern tropical North Pacific Ocean water
395 column. *Journal of Geophysical Research-Biogeosciences.*, 120(6), 1078–1092.
396 <https://doi.org/10.1002/2014JG002900>

397 Penning, H., Plugge, C. M., Galand, P. E., & Conrad, R. (2005). Variation of carbon isotope
398 fractionation in hydrogenotrophic methanogenic microbial cultures and environmental samples
399 at different energy status. *Global Change Biology*, 11(12), 2103-2113.
400 <https://doi.org/10.1111/j.1365-2486.2005.01076.x>

401 Radajewski, S., Ineson, P., Parekh, N. R., & Murrell, J. C. (2000). Stable-isotope probing as a
402 tool in microbial ecology. *Nature*, 403(6770), 646-649. <https://doi.org/10.1038/35001054>

403 Robertson, D. E. (1968). Role of contamination in trace element analysis of sea water. *Analytical*
404 *Chemistry*, 40(7), 1067-1072, <https://doi.org/10.1021/ac60263a004>.

405 Rona, P., Guida, V., Scranton, M., Gong, D. L., Macelloni, L., Pierdomenico, M., et al. (2015).
406 Hudson submarine canyon head offshore New York and New Jersey: A physical and
407 geochemical investigation. *Deep-Sea Research Part II-Topical Studies in Oceanography*,
408 121(SI), 213–232, <https://doi.org/10.1016/j.dsr2.2015.07.019>.

409 Ruppel, C. D. & Kessler, J. D. (2017). The Interaction of Climate Change and Methane
410 Hydrates. *Reviews of Geophysics*, 55(1), 126-168. <https://doi.org/10.1002/2016RG000534>

411 Skarke, A., Ruppel, C., Kodis, M., Brothers, D., & Lobecker, E. (2014). Widespread methane
412 leakage from the sea floor on the northern US Atlantic margin. *Nature Geoscience*, 7(9), 657-
413 661. <https://doi.org/10.1038/NGEO2232>

414 Summons, R. E., Jahnke, L. L., & Roksandic, Z. (1994). Carbon isotopic fractionation in lipids
415 from methanotrophic bacteria: relevance for interpretation of the geochemical record of
416 biomarkers. *Geochimica et Cosmochimica Acta*, 58(13), 2853-2863.
417 [https://doi.org/10.1016/0016-7037\(94\)90119-8](https://doi.org/10.1016/0016-7037(94)90119-8)

418 Valentine, D. L., Chidthaisong, A., Rice, A., Reeburgh, W. S., & Tyler, S. C. (2004). Carbon and
419 hydrogen isotope fractionation by moderately thermophilic methanogens. *Geochimica et*
420 *Cosmochimica Acta*, 68(7), 1571-1590. <https://doi.org/10.1016/j.gca.2003.10.012>

421 Valentine, D. L., Kessler, J. D., Redmond, M. C., Mendes, S. D., Heintz, M. B., Farwell, C., et
422 al. (2010). Propane Respiration Jump-Starts Microbial Response to a Deep Oil Spill. *Science*,
423 330(6001), 208-211. <https://doi.org/10.1126/science.1196830>

424 Wankel, S. D., Huang, Y., Gupta, M., Provencal, R., Leen, J. B., Fahrland, A., et al. (2013).
425 Characterizing the Distribution of Methane Sources and Cycling in the Deep Sea via in Situ
426 Stable Isotope Analysis. *Environmental Science & Technology*, 47(3), 1478-1486.
427 <https://doi.org/10.1021/es303661w>

428 Weinstein, A., Navarrete, L., Ruppel, C., Weber, T. C., Leonte, M., Kellermann, M. Y., et al.
429 (2016). Determining the flux of methane into Hudson Canyon at the edge of methane clathrate
430 hydrate stability, *Geochemistry, Geophysics, Geosystems*, 17(10), 3882-3892.
431 <https://doi.org/10.1002/2016GC006421>

432 Whiticar, M. J. (1999). Carbon and hydrogen isotope systematics of bacterial formation and
433 oxidation of methane, *Chemical Geology*, 161(1-3), 291-314. [https://doi.org/10.1016/S0009-2541\(99\)00092-3](https://doi.org/10.1016/S0009-2541(99)00092-3)

435